International Journal of Biological Macromolecules 93 (2016) 381–389

Contents lists available at ScienceDirect

International Journal of Biological Macromolecules

journal homepage: www.elsevier.com/locate/ijbiomac

Chitosan-modified PLGA polymeric nanocarriers with better delivery potential for tamoxifen

Chanchal Kiran Thakur[a], Nagarani Thotakura[a], Rajendra Kumar[b], Pramod Kumar[a], Bhupinder Singh[b,c], Deepak Chitkara[d], Kaisar Raza[a,*]

[a] Department of Pharmacy, School of Chemical Sciences and Pharmacy, Central University of Rajasthan, Bandar Sindri, Dist. Ajmer 305 817, Rajasthan, India
[b] UGC-Centre of Excellence in Applications of Nanomaterials, Nanoparticles and Nanocomposites, Panjab University, 160 014 Chandigarh, India
[c] Division of Pharmaceutics, University Institute of Pharmaceutical Sciences, Panjab University, 140 604 Chandigarh, India
[d] Department of Pharmacy, Birla Institute of Technology and Science (BITS)—Pilani, Vidya Vihar Campus, Pilani 333031, Rajasthan, India

ARTICLE INFO

Article history:
Received 27 May 2016
Received in revised form 20 August 2016
Accepted 28 August 2016
Available online 29 August 2016

Keywords:
Nanocarriers
Nanotechnology
Dermatokinetics
Bioavailability
Cytotoxicity
Confocal laser scanning microscopy
Cellular uptake

ABSTRACT

Breast cancer is believed as the second most common cause of cancer-related deaths in women for which tamoxifen is frequently prescribed. Despite many promises, tamoxifen is associated with various challenges like low hydrophilicity, poor bioavailability and dose-dependent toxicity. Therefore, it was envisioned to develop tamoxifen- loaded chitosan-PLGA micelles for potential safe and better delivery of this promising agent. The chitosan-PLGA copolymer was synthesised and characterised by Fourier Transform-Infrared, Ultraviolet-visible and Nuclear Magnetic Resonance spectroscopic techniques. The drug-loaded nanocarrier was characterised for drug-pay load, micrometrics, surface charge and morphological attributes. The developed system was evaluated for *in-vitro* drug release, haemolytic profile, cellular-uptake, anticancer activity by cytotoxicity assay and dermatokinetic studies. The developed nano-system was able to substantially load the drug and control the drug release. The *in-vitro* cytotoxicity offered by the system was significantly enhanced *vis-a-vis* plain drug, and there was no substantial haemolysis. The IC_{50} values were significantly decreased and the nanocarriers were uptaken by MCF-7 cells, noticeably. The carrier was able to locate the drug in the interiors of rat skin in considerable amounts to that of the conventional product. This approach is promising as it provides a biocompatible and effective option for better delivery of tamoxifen.

1. Introduction

Nanotechnology is associated with designing useful materials, devices and systems through control of matter on the micromeritic level, and exploitation of novel phenomena and properties at the length scale [1,2]. In the present era, nanotechnology is a rapidly emerging area, especially in medical research, which is focusing on development of nanoparticles/nanocarriers for diagnostic and therapeutic applications [3]. Nanotechnology-based carriers are being employed for the targeted drug delivery. The important examples of such carriers are liposomes, ethosomes, niosomes, polymeric micelles, solid-lipid nanoparticles, nanospheres, carbon nanotubes, C_{60}-fullerenes and nanocapsules [4–6]. Among all these nanocarriers, polymeric micelles are established for prolonged blood circulation, enhanced permeation and retention (EPR) effect *via* tumor vessels, better delivery to tumor cells, increase therapeutic efficiency and significant tumor accumulation [7]. Despite all these, preparations of polymeric micelles emerge to be relatively simple as compared to other novel drug delivery systems [8]. These carriers can easily load various poorly soluble drugs and can enhance the bioavailability of such drugs [9].

Tamoxifen (TAM) is a cytostatic drug and is known for its anti-estrogenic nature. It is most widely used for the treatment of all stages of breast cancers, especially for metastatic breast cancers [10]. Despite its pharmacological significance, TAM is tagged with challenges like lower aqueous solubility and lower tissue selectivity. Apart from this, long-term usage of TAM puts patients at increased risk of thrombo-embolic events and uterine malignancies. The other major adverse effects of TAM include higher incidences of endometrial cancer, liver cancer and development of drug resistance [11]. In order to circumvent the systemic side

* Corresponding author at: Department of Pharmacy, School of Chemical Sciences and Pharmacy, Central University of Rajasthan, Bandar Sindri, Distt. Ajmer 305 817, Rajasthan, India.
E-mail addresses: drkaisar@curaj.ac.in, razakaisar_pharma@yahoo.co.in (K. Raza).

http://dx.doi.org/10.1016/j.ijbiomac.2016.08.080
0141-8130/

effects, TAM can be successfully delivered to the targeted cancer sites employing topical route. The challenges of TAM by oral route (cytotoxicity, first-pass metabolism and hypercalcemia) and parenteral route (solubility and tissue necrosis) can be by-passed using topical administration [12].

Poly (lactic-co-glycolic) acid (PLGA) has been approved by United States-Food and Drug Administration, European Medicine Agency (EMA) and other federal agencies for delivery of drugs in humans, due to its biodegradability, biocompatibility and immune neutral properties [13,14]. PLGA is one of the most widely used biodegradable polymers, as it undergoes hydrolysis in the body to produce biodegradable and biocompatible metabolic monomers, i.e. lactic acid and glycolic acid. These metabolites are consumed in citric acid cycle [15]. On the other hand, chitosan (CS) is a semi-processed natural cationic linear polysaccharide, composed of (1 → 4) linked glucosamine units, with some proportion of *N*-acetyl-glucosamine [16]. CS has a variety of promising pharmaceutical uses and is presently considered as a novel material in drug delivery systems, wound healing, microbiology and medicinal devices, and also the polymer is known for its hypo-cholesterolemic effects [15]. CS is non-toxic and non-immunogenic, polysaccharide with an ability to enhance the penetration of large molecules across mucosal surfaces [15]. Henceforth, it was envisioned to develop a copolymer with merits of both PLGA and CS, and encapsulate the drug in micelles composed of CS-PLGA copolymer for better drug delivery promises.

2. Materials and methods

2.1. Materials

Poly (lactic-co-glycolic acid) (PLGA; 75:25; M_W ~90,000; RESOMER® RG 752S) was supplied as gift sample from M/s Evonik Nutrition & Care GmbH (Darmstadt, Germany). Chitosan (CS) and dialysis membrane were procured from M/s Himedia laboratories (P) Ltd. (Mumbai, India). Tamoxifen (TAM) was purchased from M/s Sigma-Aldrich chemicals (P) Ltd (Bangalore, India). *N, N*-dicyclohexyl carbodiimide (DCC) and dimethyl sulphoxide (DMSO) were purchased from M/s Spectrochem (P) Ltd. (Mumbai, India). Methylene chloride (DCM), citric acid, dipotassium hydrogen phosphate, disodium hydrogen phosphate, potassium dihydrogen phosphate and sodium hydroxide were purchased from M/s Central Drug House (P) Ltd. (New Delhi, India). Conc. nitric acid was procured from M/s Molychem industries (Mumbai, India). Tween 80 was supplied by M/s Fisher Scientific (P) Ltd (Mumbai, India). MCF-7 cell lines were provided by The National Centre for Cell Science, Pune, India. Distilled water was employed throughout the studies.

2.2. Methods

2.2.1. Synthesis of chitosan-PLGA copolymer

Synthesis of CS-PLGA copolymer was possible due to reaction between free carboxylic acid groups of PLGA with amino groups of CS by means of coupling agent, i.e., DCC. The reaction scheme has been shown in Fig. 1. CS solution was prepared by dissolving CS (0.1 g) in 2 mL of concentrated nitric acid, which was further diluted to 20 mL with distilled water. PLGA solution was prepared by dissolving both PLGA (0.1 g) and DCC (1 g) in 11.5 mL of DCM at 60 °C for 10–20 min. The resulting PLGA solution was drop-wise added to CS solution, with continuous stirring. The resulting system was further subjected to dialysis in distilled water for 24 h. CS-PLGA copolymer was harvested by removing the solvent using rotatory evaporation [17].

2.2.2. Preparation of chitosan-PLGA polymeric micelles

Initially, both TAM (10 mg) and copolymer (20 mg) were dissolved in 3 mL of DMSO and filled into a syringe. This DMSO solution was added drop wise with continuous stirring into beaker containing 10 mL mixture of phosphate buffered solution (PBS) of pH 7.4 and 2 mL of Tween-80 at 60 °C. The resultant dispersion was subjected to sonication for 1 h. Sonicated dispersion was filtered using Whatman filter paper (0.22 μm). Obtained polymeric micelles were stored in refrigerator till further use. Blank micelles without TAM were also prepared by same method [7,18].

2.3. Characterization of copolymer and polymeric micelles

2.3.1. FT-IR spectrum

Structural analysis of compounds was performed by Fourier Transform Infrared Spectroscopy (FT-IR). The samples were punched into pellets with potassium bromide. FT-IR data were recorded at a wave number range of 4000–400 cm^{-1}

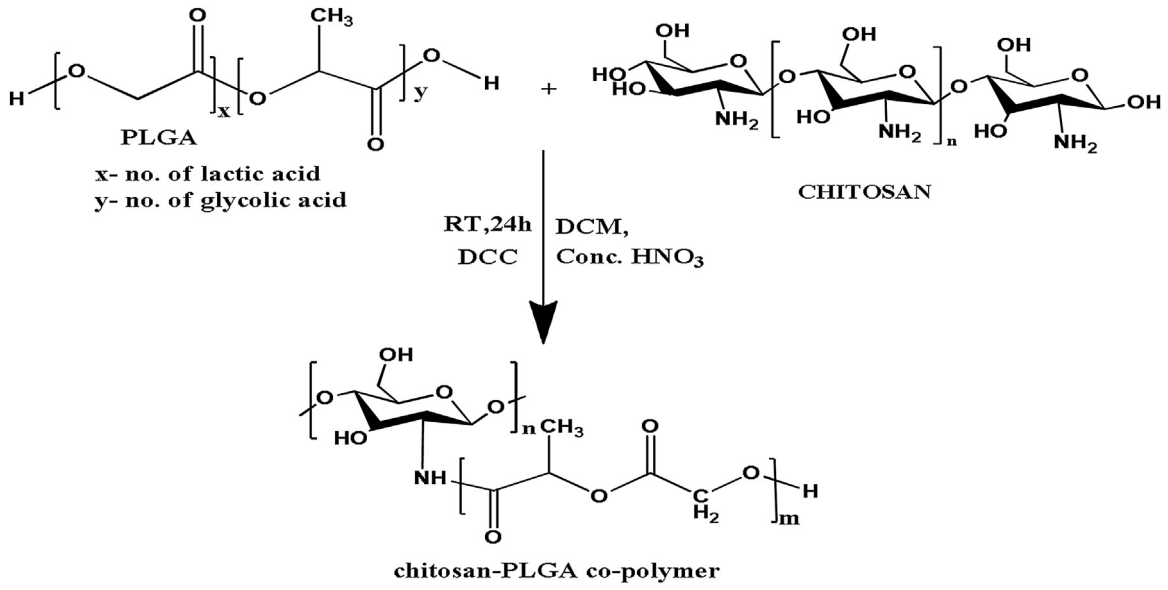

Fig. 1. Synthetic scheme for synthesis of chitosan-PLGA copolymer.

using FT-IR Spectrometer (Spectrum two, M/s Perkin Elmer Co., Waltham, Massachusetts, USA).

2.3.2. NMR spectrum

The ^{1}H NMR spectrum of CS-PLGA conjugate was recorded using nuclear magnetic resonance spectrometer (ASCEND 500WB NMR Spectrometer, M/s Bruker Bio Spin Corporation., Indiana, USA). CS-PLGA saturated solution was prepared in deuterated DMSO and scanned for the NMR spectrum.

2.3.3. Molar mass determination

Gel permeation chromatography (GPC) was employed to determine molecular weight of the polymer. Tetrahydrofuran (THF; HPLC grade) was used as the mobile phase, filtered through 0.22 μm filter paper and deaerated in ultrasonic bath for 30 min. Polystyrene standards and test samples were prepared by dissolving 1 mg of the polymer in 1 mL of THF (HPLC grade), filtered through 0.22 μm filter paper and analyzed using Waters GPC system coupled with refractrometer 2414. Chromatographic separation was done on Water's styragel column in an isocratic mode with the stated mobile phase at a flow rate of 1 mL/min. The sample injection volume was kept at 50 μL. The data was analyzed using "Breeze 2- Add on" software [19].

2.3.4. CMC (Critical micellar concentration) determination

CMC was determined by using iodine/potassium iodide method. Solution of 250 mg of I_2 and 500 mg of KI were dissolved in 25 mL of DCM. All the dilutions (1–10 μg/mL) prepared were incubated for overnight by adding 25 μL of iodine solution. Incubated solutions were analyzed using UV–vis spectrophotometer at a wavelength of 366 nm. A graph was plotted between concentration of polymer taken and absorbance observed. The point at which there is a sharp increase in absorbance was CMC value [17].

2.3.5. Particle size distribution and zeta potential studies

Particle size and poly-dispersity index values were determined by dispersing the prepared polymeric micelles in PBS 7.4 (1 mg/mL) and analysing the same on Malvern Zetasizer (M/s Malvern, Worcestershire, UK) installed at BITS, Pilani, India. The same equipment was employed for the determination of zeta-potential values. Average value from three repeated observations was reported as the final result.

2.3.6. Morphology

Morphological evaluation was conducted using transmission electron microscopy (TEM) installed at Central Instrumentation Laboratory, Panjab University, Chandigarh, India. In this process, one drop of polymeric micellar dispersion was added with 1% aqueous solution of phosphotungstic acid on carbon film coated copper grid and the image was clicked at suitable magnification.

2.3.7. Entrapment and drug loading studies

Entrapment efficacy (EE) and drug loading (DL) values were determined using filtration method. The residue of Section 2.2.2 was used for the study. Filter paper was extracted in methanol and analyzed spectrophotometrically for unentrapped drug. Sample from blank micelles, treated analogously, served as the blank [20].

2.4. Evaluation studies

2.4.1. In-vitro drug release studies

Pure TAM and CS-PLGA based TAM-loaded polymeric micelles (equivalent to 1 mg of TAM) were weighed and packed into dialysis bags. These dialysis bags were suspended in 30 mL solution of methanol and PBS of pH 5.6/pH 6.8/pH 7.4 (1:9 v/v ratio) [21]. Temperature was maintained at 37 ± 1 °C with continuous stirring. Samples of 2 mL each were collected at regular intervals. Equal volume of fresh diffusion medium was replaced to maintain the sink conditions, after each sample. The samples were analysed by UV spectrophotometer for the drug content.

2.4.2. Ex-vivo hemolysis studies

This protocol was executed on whole human blood samples. The study was duly approved by the *Institutional Ethics Committee*, Central University of Rajasthan, Bandar Sindri, Kishangarh, Ajmer, India. In brief, 2 mL of blood sample was collected from healthy male human volunteer in a vial containing 124 mmol/L of sodium citrate solution. With the help of centrifugation, erythrocytes were separated and washed with normal saline. These washed erythrocytes were re-suspended in normal saline (2 mL). Test formulations, i.e., TAM plain and TAM-loaded polymeric micelles (equivalent of 1 mg of TAM) were added to 1 mL of RBC dispersion. On the other hand, the reference dispersion was prepared by dispersing erythrocytes in distilled water. All these test tubes were incubated at 37 °C for 1 h. After incubation, centrifugation (2000 × g) was performed for 5 min to harvest the transparent supernatant. The supernatant was analyzed using UV–vis spectroscopy at λ_{max} of 415 nm and the hemolysis induced by distilled water was taken as 100% [22].

2.4.3. Protein binding studies

A 2% w/w bovine serum albumin (BSA) solution was prepared in PBS 7.4. TAM encapsulated CS-PLGA micelles (drug equivalent to 1 mg) and pure TAM (1 mg) were weighed and dispersed in 1 mL of BSA solution. The dispersions were packed in dialysis bags, separately. The dialysis bags were suspended in 20 mL of PBS 7.4. Samples were withdrawn after 1 h, 2 h, 4 h and 6 h, were analyzed by UV–vis spectrophotometer [23].

2.4.4. In-vitro cytotoxicity assay

Human breast cancer MCF-7 cells were fed in 96-welled plate with 5% CO_2. The samples of pure TAM and TAM-loaded micelles in various concentrations were added to these wells and incubated for 24 h at 37 °C. Solution of MTT (5 mg/mL), 10 μL was added to each well and incubation was done for 4 h. The developed formazan crystals were dissolved in 200 μL of DMSO. The absorbance was recorded at 570 nm using ELISA reader [24].

2.4.5. Confocal laser scanning microscopy

MCF-7cells with a density of approx. 15,000 cells/cm^2 were seeded on petri-plates. The drug-loaded micelles were tagged with coumarin-6. The dye-tagged nanocarriers were added to the cell culture medium. The incubation was done at 37 °C for 24 h. Cells were washed using PBS 7.4. Cell fixing was done using ice cold methanol, followed by washing with PBS 7.4. Nucleus staining was done with 300 nM solution of DAPI for 5 min. The cells were scanned under confocal laser scanning microscope (Nikon C2 Plus, with NIS Elements Version 4.3 Software). For DAPI, the wavelengths used were 405 nm and 417–477 nm, whereas for coumarin-6 laser wavelengths used were 488 nm and 500–550 nm, respectively for excitation and emission. Cells with fluorescent nuclei (blue stained) and drug-invaded regions (green-stained) were captured at 60× magnification. Experiments were performed in triplicate.

2.4.6. Dermatokinetic studies

Skins of Wistar rats were used for this study. The animal protocols were duly approved by *Institutional Animal Ethics Committee*, Panjab University, Chandigarh, India. After sacrificing the animals, the hair on the dorsal side of animals were removed. The skin was harvested, discharged of adhering fat layers, and mounted on Franz diffusion cells (M/s Permegear, Inc., PA, USA), having a cross-sectional area of 3.142 cm^2 and receptor volume of 30.0 mL.

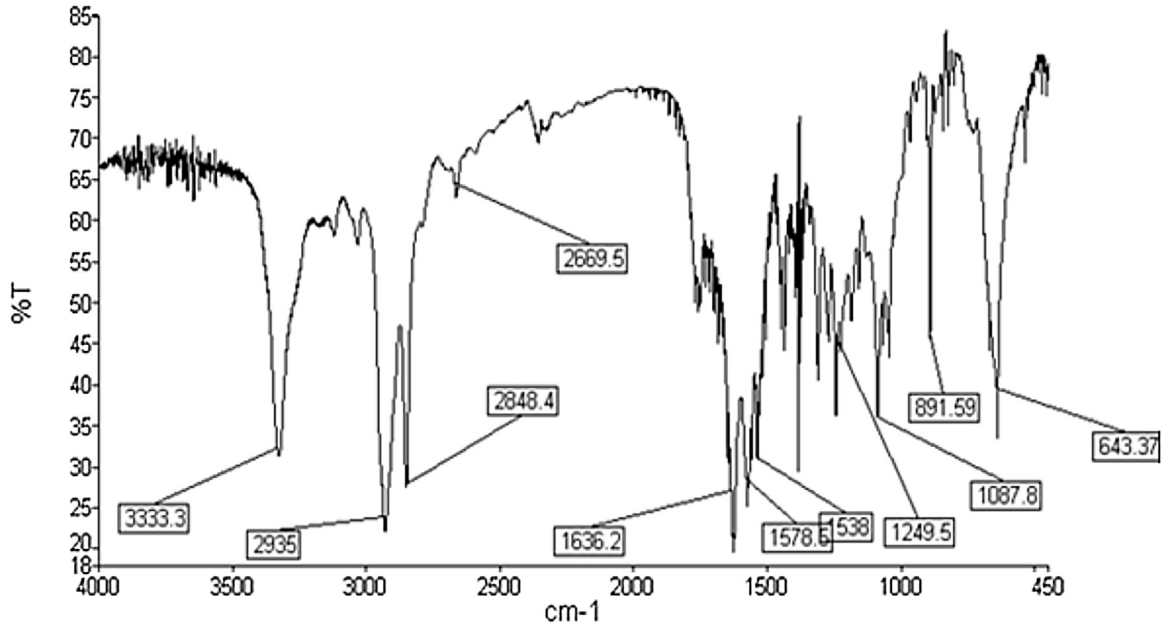

Fig. 2. FT-IR spectrum of chitosan-PLGA copolymer.

The diffusion medium in the receptor compartment was composed of methanol: PBS 7.4 mixture in 1:9 v/v ratios. The assembly was maintained at 35 ± 1 °C with the help of thermo-regulated outer water jacket, while the diffusion medium was stirred continuously using a magnetic stirrer. In this case, the whole skin was removed from the Franz cell at the respective sampling time. The skin was washed thrice to remove any adhering formulation and subsequently soaked in hot water (60 °C) to separate the epidermis from dermis. Both of the sections were chopped into small pieces, separately, and extracted in methanol (5 mL) for 24 h. After filtering the solution through a membrane (0.45 μm), the filtrate was analyzed using the RP-HPLC technique[20].

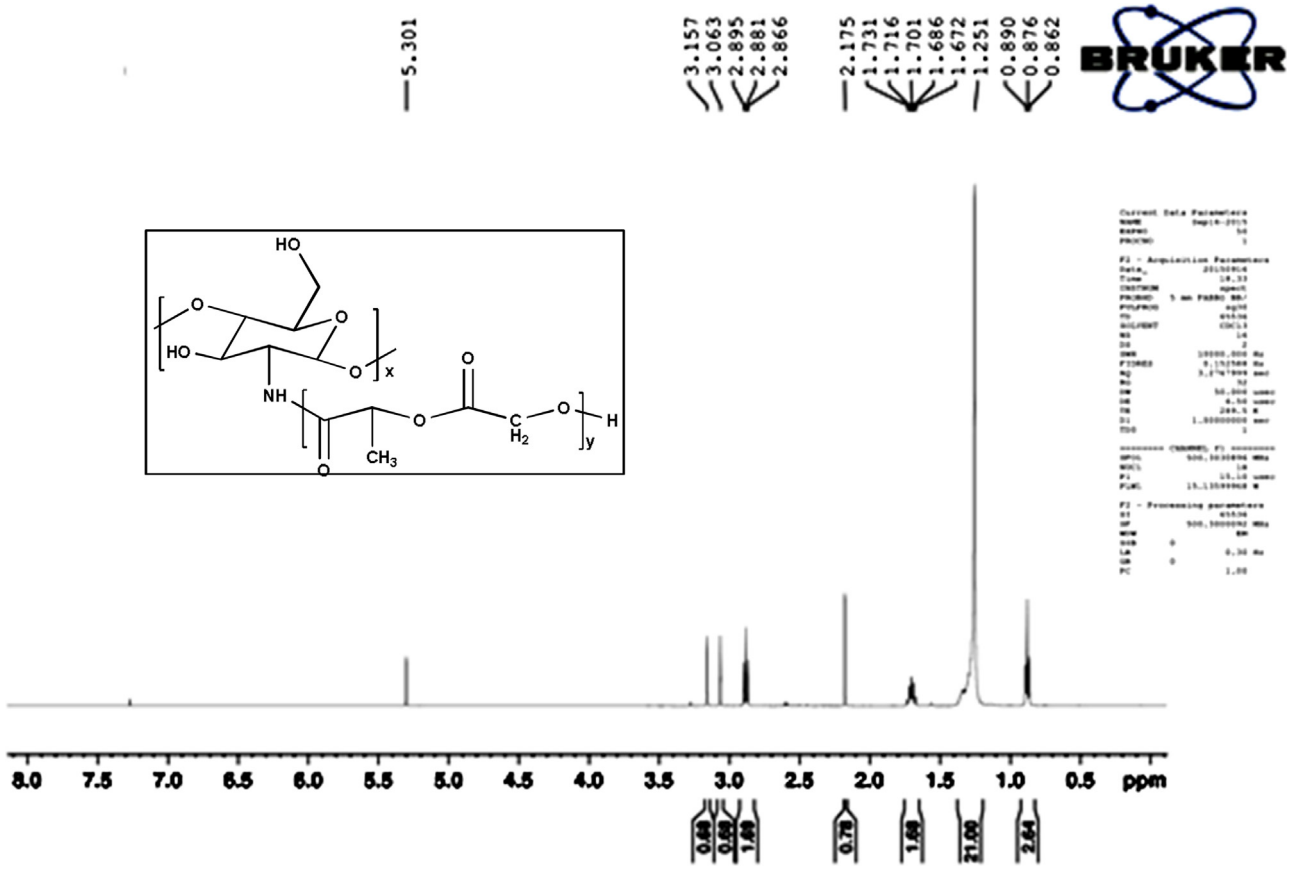

Fig. 3. ^{1}H NMR Spectrum of chitosan-PLGA copolymer.

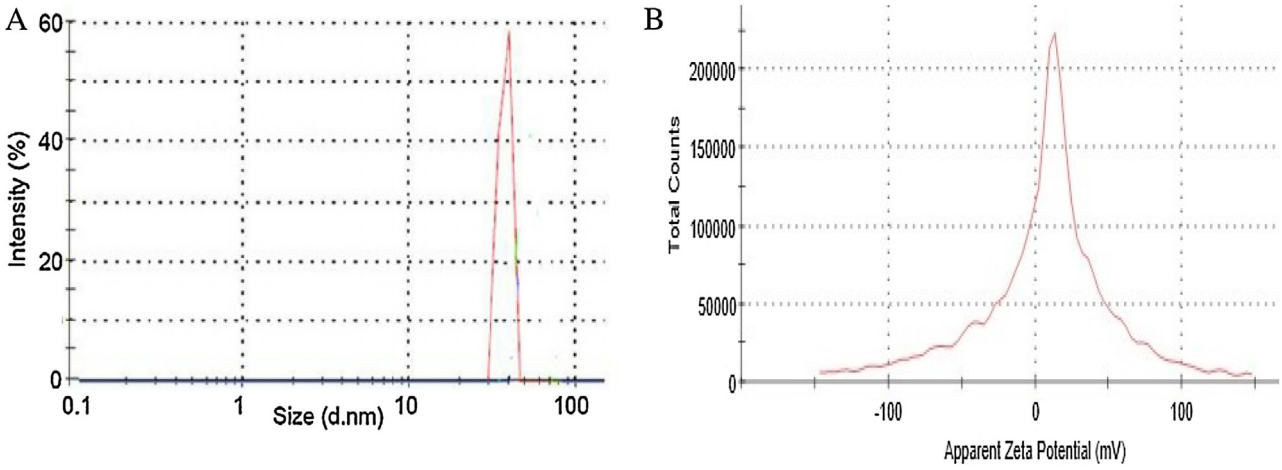

Fig. 4. Graphs of (A) Particle size and (B) Zeta potential of drug-loaded micelles.

3. Results and discussion

3.1. Characterization studies

3.1.1. FT-IR of chitosan-PLGA copolymer

Fig. 2 represents FT-IR spectrum of CS-PLGA copolymer, which confirmed the formation of amide (—CO—NH) bond between amine ($—NH_2$) group of CS and free carboxylic acid (—COOH) group of PLGA. The peak at 3333.3 cm^{-1} represented —N—H stretching, where as the peak at 1636.2 cm^{-1} represented the presence of C=O group of amide. Peaks at 2935 cm^{-1}, 2848.4 cm^{-1} and 2669.5 cm^{-1} could be attributed to presence of C—H stretching and peak at 1578.6 cm^{-1} represented the N—H bend. However, the peak at 1249.5 cm^{-1} and 1087.8 cm^{-1} inferred the presence of C—O of CS and PLGA.

3.1.2. NMR of chitosan-PLGA copolymer

Through ^1H nuclear magnetic resonance (NMR) spectrum, it was speculated that the structure of CS-PLGA copolymer contained amide bond (—CO—NH—). In Fig. 3 peaks at δ 5.301, indicate the

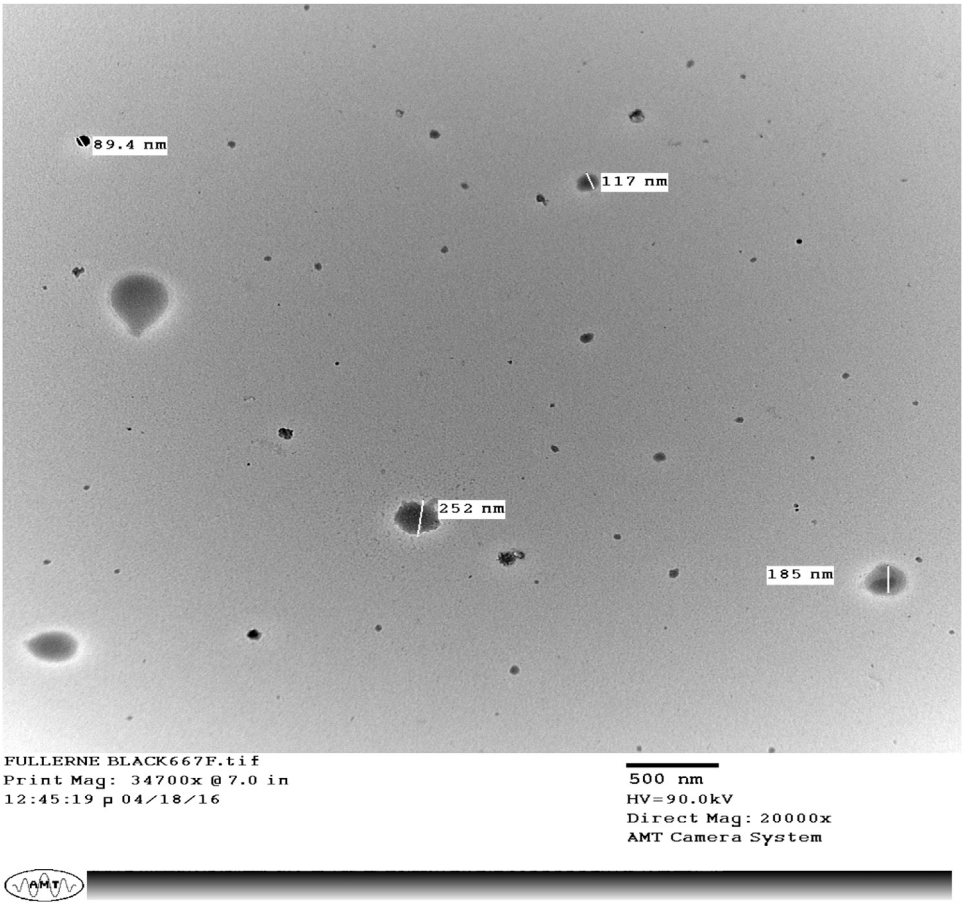

Fig. 5. TEM microphotograph of drug-loaded micelles.

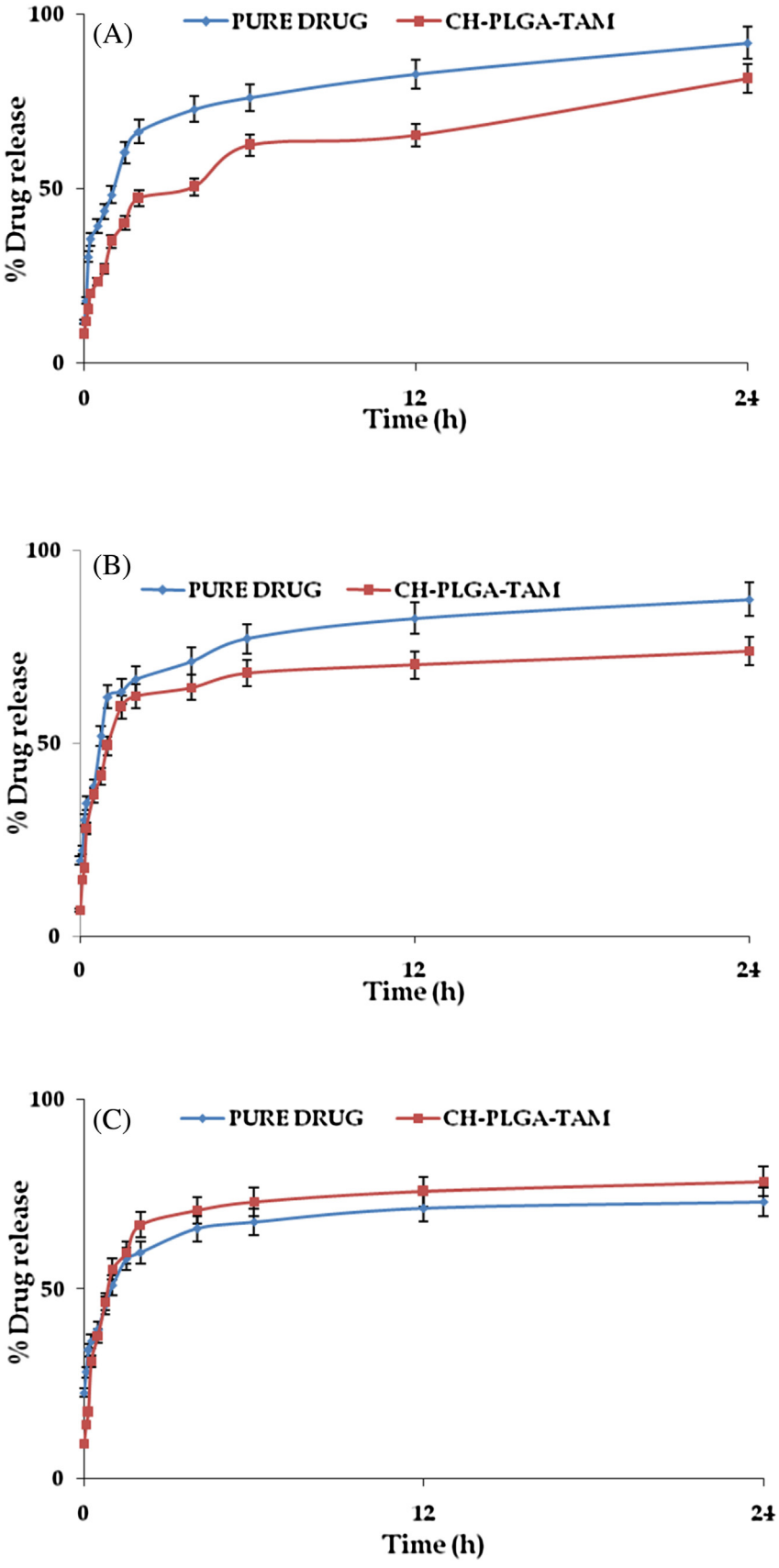

Fig. 6. Graph showing the drug release pattern of pure TAM and TAM-loaded polymeric micelles at (A) pH 5.6, (B) pH 6.8, (C) pH 7.4.

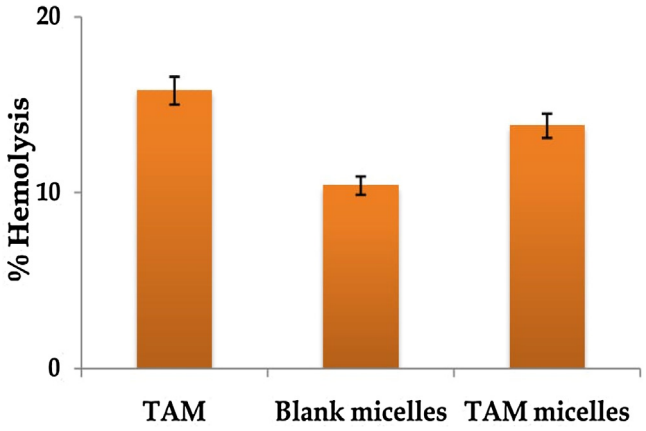

Fig. 7. Bar graph showing% hemolysis induced by the studied systems.

proton of amide (R—CO—N—**H**), and peaks at δ 1.731, δ 1.716, δ 1.701, δ 1.686, δ 1.672 indicated the presence of methyl group (—CH_3) of PLGA. The δ values at 2.866, 2.881, and 2.895 indicated the presence of methoxy group (—CH_2—O—) of CS and PLGA. From the spectrum, it was concluded that CS-PLGA copolymer was successfully synthesised.

3.1.3. Molar mass and CMC

From GPC, the number average molecular weight (M_n) and the weight average molecular weight (M_w) of the graft copolymer came out to be 786287 Da and 807459 Da, respectively with a PDI value of 1.03. The data inferred that the developed copolymer was graft copolymer, not a block copolymer. CMC value was calculated as 3.2 μg/mL after plotting a graph between concentrations of copolymer containing the I_2/KI and the corresponding absorbance. The findings are in consonance with the CMC reports on copolymers involving PLGA [7].

3.1.4. Particle size and zeta potential studies

The observed average size of blank micelles was 36.48 nm and that of drug-loaded micelles was 81.48 nm. It can be inferred that the drug was encapsulated successfully in micelles, resulting in increase of the average size. PDI values were observed as 0.307 and 0.209 for blank micelles and TAM-loaded micelles, respectively. PDI values were less than 0.3, indicating substantial homogeneity in studied dispersion [21]. The zeta-potential values of blank as well as drug-loaded micelles were towards positive side. For blank micelles, the observed zeta-potential was +14.93 ± 2.11 mV and for drug-loaded micelles, the value was +19.27 ± 4.34 mV. Similar findings are characteristic for positively charged CS-based nanocarriers [25]. However, enhancement in positive charge, after incorporation of TAM, can be ascribed to the presences of protonated TAM in the micellar structures [26]. Fig. 4 represents the graphs for both particle size and zeta potential of drug-loaded micelles.

Table 1
Various dermatokinetic parameters of TAM topical formulations in epidermis and dermis of Wistar rats (n = 3).

Dermatokinetic Parameter	TAM		TAM-micelles	
	epidermis	dermis	epidermis	dermis
$AUC_{0\text{-}8h}$ (μg cm^{-2} h)	140.60	99.59	339.51	218.15
Tmax (h)	0.22	0.19	0.43	0.23
Kp (h^{-1})	3.51	4.23	4.95	5.68
Ke (h^{-1})	0.31	0.45	0.10	0.23
C_{max} (μg cm^{-2})	32.30	29.40	110.30	59.70

3.1.5. Morphology study (TEM)

Fig. 5 shows the TEM microphotograph of polymeric micelles. It is vivid that the micelles were present in segregation, devoid of any evidence of agglomeration. The developed systems were spherical in shape, as it is expected from such carriers.

3.1.6. Entrapment Efficacy(EE) and drug loading (DL) studies

The observed EE and DL values of TAM-loaded micelles were as 89.78 ± 7.31% and 45 ± 4.24%, respectively. The carrier offered substantial amount of drug loading (>10%), even in 1:2 mass ratio. Henceforth, the developed systems can be regarded as an ideal option to load chemotherapeutic agents in the desired higher doses.

3.2. Evaluation studies

3.2.1. In-vitro Drug Release Studies

Drug release pattern of TAM and the TAM-loaded micelles was studied in 3 different pH (5.6, 6.8 and 7.4), and it is confirmed from Fig. 6 that the release of drug from polymeric micelles was sustained as compared to pure TAM. Interestingly, more drug release was observed at cancer cell pH of 5.6 and least at plasma pH of 7.4 from the drug-loading micelles. However, there was no such distinction of release pattern in plain drug. This finding is unique and of significance, as it was ensured that the drug will be released at the target site, not in plasma [27].

3.2.2. Ex-vivo hemolysis studies

From Fig. 7 it was observed that there was significant difference between the hemolytic profile of pure drug and developed colloidal system. Significant hemolysis by TAM can be ascribed to the positive charge of protonated drug. But from Fig. 7, it was clear that hemolytic activity of drug-loaded micelles was lower than the

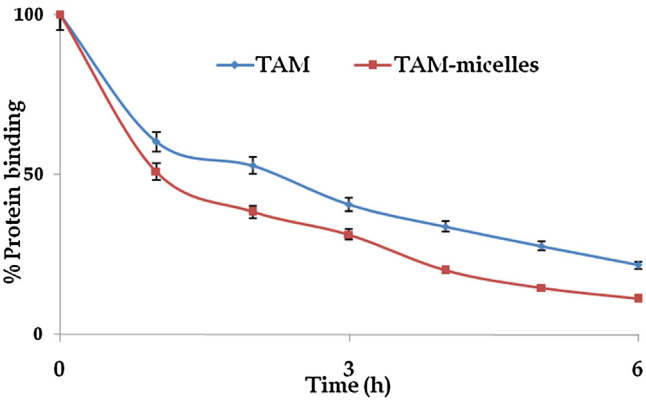

Fig. 8. Graph showing% protein binding of TAM and TAM-loaded polymeric micelles.

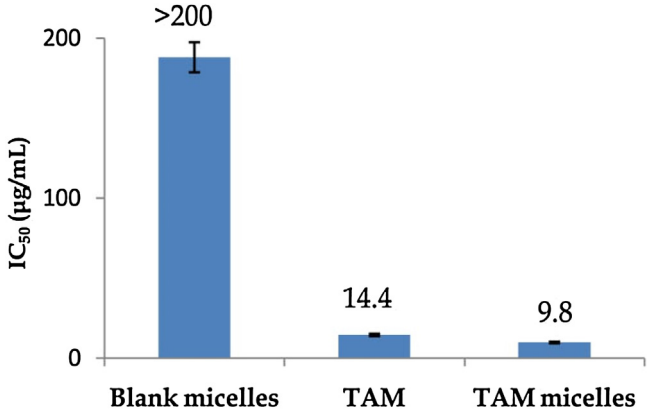

Fig. 9. Bar diagram for IC_{50} values of blank micelles, TAM and TAM-loaded micelles.

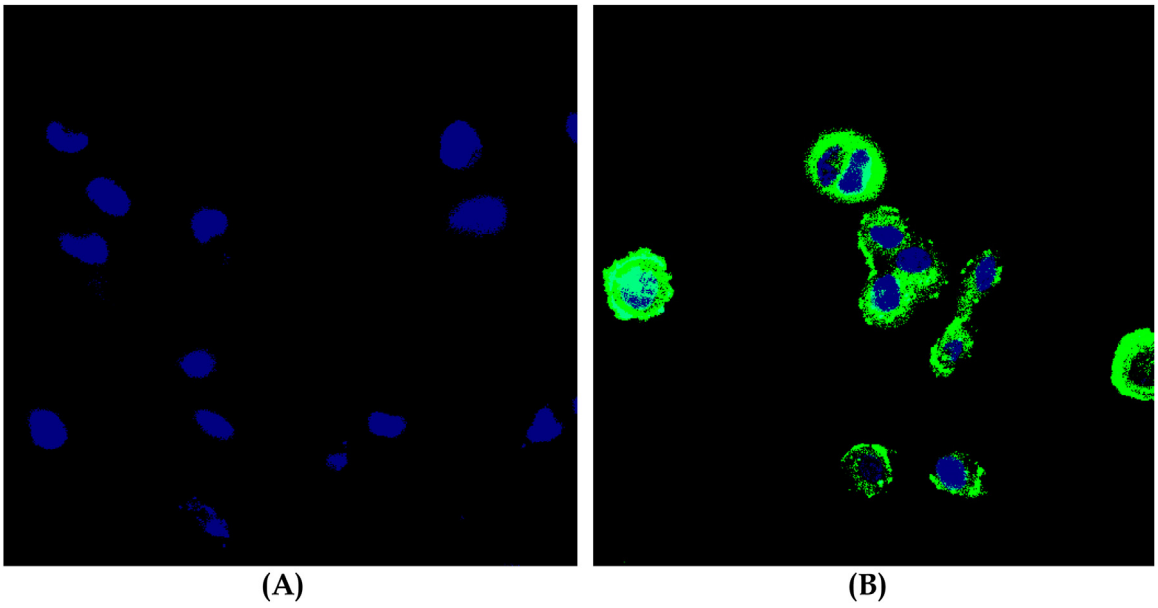

Fig. 10. Confocal laser scanning microphotographs (60×) of: (A) Control with stained nuclei; (B) CS-PLGA treated MCF-7 cells.

plain drug. Surprisingly, blank micelles offered significantly lower hemotoxicity, plausibly due to nullification of charge by reaction between positively charged CS and negatively charged PLGA [28]. On the other hand, the drug-loaded system was able to enhance the hemo-compatibility of the hemolytic drug, which can be viewed as a positive drug delivery outcome.

3.2.3. Protein binding

Fig. 8 shows the% protein binding of TAM and TAM-loaded micelles at different time intervals of 0–6 h. At all the studied points, it was observed that the protein binding of the drug from prepared micelles was substantially lower than that of the plain drug. At 1 h, the protein binding of pure TAM was approx. 62%, where as it was around 50% for the micelle-loaded drug. The findings indicate that electrostatic interaction between the positively charged micelles and negatively charged BSA was not of significance for the binding profile. This decreased protein binding gives promise of better availability of drug to the target site than that of the plain drug [29].

3.2.4. In vitro cell cytotoxicity studies

As shown in Fig. 9, IC_{50} value of TAM was substantially decreased after incorporation into the micelles. As TAM belongs to BCS class II, the drug itself inherits better permeation. But after incorporation into CS-PLGA polymeric micelles, permeation ability was further increased along with adhesion property on the membranes of the cells. The plausible better permeation and subsequent release of drug in the interiors of cancer cells might have resulted in better cytotoxicity [30].

3.2.5. Confocal laser scanning microscopy

Fig. 10 represents microphotographs obtained from confocal laser scanning microscopy. These images show that prepared micelles were able to invade the cytoplasm as well as interiors of the nuclei of cells, whereas plain dye was not able to achieve the same. Green fluorescence shows that coumarin-6 tagged micelles were able to penetrate into cells and the blue stains shows DAPI stained nuclei. These images provide better support for *in vitro* cytotoxicity results as it is vivid that the micelles were able to get the access of cytoplasm and nucleus easily. As the cells were ER+ in nature, and provided a better understanding of the cytotoxicity induced by positively-charged TAM-loaded micelles [31].

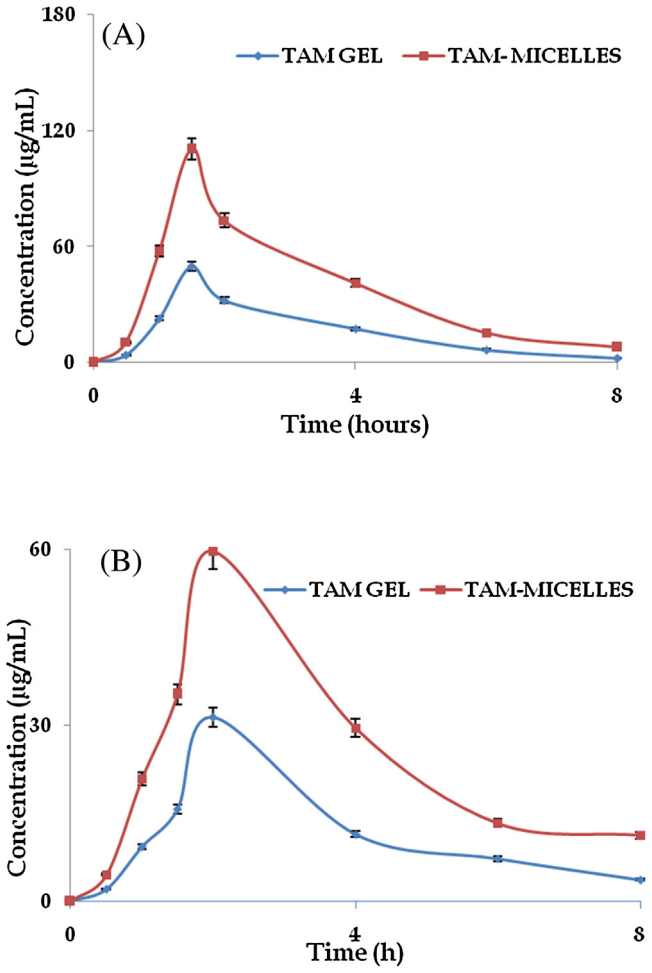

Fig. 11. (A) Graph showing the amount of drug present in the epidermis of Wistar rats a various time points. (B) Graph showing the amount of drug presents in the dermis of Wistar rats a various time points.

3.2.6. Dermatokinetic studies

Fig. 11 represents the graph showing the sojourn of drug in epidermis and dermis as a function of time by both pure TAM and TAM-loaded polymeric micelles. It was clear that the developed polymeric micelles were able to deliver more amount of drug to dermis and epidermis in comparison to pure drug. The various dermatokinetic parameters calculated as per 1 CBM per oral model have been tabulated in Table 1. The bioavailability of drug in epidermis was enhanced by approx. 3.5 folds *vis-à-vis* plain drug, whereas the enhancement in dermis was approx. 2.2 times. The absorption in both dermis and epidermis was enhanced, whereas the elimination of the drug was retarded in both the skin layers by the strategically-designed micelles. The C_{max} values were also of higher magnitude in both the layer for the TAM-loaded micelles to that of the plain drug. The findings are encouraging as the evidence is available that the drug can be delivered to deeper layers of skin with desired rate, in substantial amounts and in higher concentrations. The results pave a path for the development of a safer and effective topical product for TAM.

4. Conclusions

In an endeavour to explore the applications of strategically-designed nanocarriers for TAM, the results are encouraging advocating enhanced efficacy, tolerability, cellular uptake and dermal/epidermal bioavailability. Such polymers offer a promise to control the drug release at near to neutral pH and enhance the same at the cancer cell pH. This unique attribute along with bioadhesion and better endocytosis to the cancer cells make such carriers as the front-runners in cancer chemotherapy, though at the pre-clinical/*in-vitro* levels. Further research employing such biocompatible and promising systems should be extrapolated on other similar chemotherapeutic agents, and the evidence generation in apt preclinical models will provide a platform for the better utilization of such systems.

Conflict of interest

The authors report no conflict of interest.

Acknowledgements

University Grant Commission, New Delhi, India is acknowledged for financial support in the form of UGC-Start-Up Grant (F.30-18/2014BSR) to the corresponding author. Dr Deepak Chitkara also acknowledges the financial support (scheme for young scientist [YSS/2014/000521]) from Science and Engineering Research Board (SERB), Department of Science and Technology, Government of India.

References

[1] I. Kaur, R. Agrawal, Nanotechnology: a new paradigm in cosmeceuticals, Recent Pat. Drug Deliv. Formul. 1 (2007) 171–182.
[2] P. Viana Baptista, Cancer nanotechnology – prospects for cancer diagnostics and therapy, Curr. Cancer Ther. Rev. 5 (2016) 80–88.
[3] A.H. Faraji, P. Wipf, Nanoparticles in cellular drug delivery, Bioorg. Med. Chem. 17 (2009) 2950–2962.
[4] K. Raza, D. Kumar, C. Kiran, M. Kumar, S.K. Guru, P. Kumar, S. Arora, G. Sharma, S. Bhushan, O.P. Katare, Conjugation of docetaxel with multiwalled carbon nanotubes and co-delivery with piperine: implications on pharmacokinetic profile and anti-cancer activity, Mol. Pharm. 13 (2016) 2423–2432.
[5] K. Raza, M. Kumar, P. Kumar, R. Malik, G. Sharma, M. Kaur, O.P. Katare, Topical delivery of aceclofenac: challenges and promises of novel drug delivery systems, Biomed Res. Int. 2014 (2014) 1 (Article ID 406731,ages).
[6] P. Kumar, K. Raza, L. Kaushik, R. Malik, S. Arora, O.P. Katare, Role of colloidal drug delivery carriers in taxane-mediated chemotherapy: a review, Curr. Pharm. Des. (2016), http://dx.doi.org/10.2174/1381612822666160524144926.
[7] K. Raza, N. Kumar, C. Misra, L. Kaushik, S.K. Guru, P. Kumar, R. Malik, S. Bhushan, O.P. Katare, Dextran-PLGA-loaded docetaxel micelles with enhanced cytotoxicity and better pharmacokinetic profile, Int. J. Biol. Macromol. 88 (2016) 206–212.
[8] N. Nishiyama, K. Kataoka, Current state achievements, and future prospects of polymeric micelles as nanocarriers for drug and gene delivery, Pharmacol. Ther. 112 (2006) 630–648.
[9] V. Mourya, N. Inamdar, Polymeric micelles: general considerations and their applications, Indian J. Pharm. Educ. Res. 45 (2011) 128–138.
[10] B. Sahana, K. Santra, S. Basu, B. Mukherjee, Development of biodegradable polymer based tamoxifen citrate loaded nanoparticles and effect of some manufacturing process parameters on them: a physicochemical and in-vitro evaluation, Int. J. Nanomed. 5 (2010) 621–630.
[11] D. Gal, S. Kopel, M. Bashevkin, J. Lebowicz, Oncogenic potential of tamoxifen on endometria of postmenopausal women with breast cancer—preliminary report, Gynecol. Oncol. 42 (1991) 120–123.
[12] B. Furr, V. Jordan, The pharmacology and clinical uses of tamoxifen, Pharmacol. Ther. 25 (1984) 127–205.
[13] I. Amjadi, M. Rabiee, M.S. Hosseini, M. Mozafari, Synthesis and characterization of doxorubicin-loaded poly(lactide-co-glycolide) nanoparticles as a sustained-release anticancer drug delivery system, Appl. Biochem. Biotechnol. 168 (2012) 1434–1447.
[14] I. Amjadi, M. Rabiee, M.S. Hosseini, F. Sefidkon, M. Mozafari, Nanoencapsulation of *Hypericum perforatum* and doxorubicin anticancer agents in PLGA nanoparticles through double emulsion technique, IET Micro Nano Lett. 8 (2013) 243–247.
[15] N. Jalali, F. Moztarzadeh, M. Mozafari, S. Asgari, S. Shokri, S.N. Alhosseini, Chitosan-surface modified poly(lactide-co-glycolide) nanoparticles as an effective drug delivery system, biomedical engineering (ICBME), 18th Iranian Conference of Tehran (2011) 109–114.
[16] N. Jalali, G. Trujillo-de Santiago, M. Motevalian, M.Y. Karimi, N.P.S. Chauhan, Y. Habibi, M. Mozafari, Chitosan-functionalized poly(lactide-co-glycolide) nanoparticles: Breaking through the brain's tight security gateway, bioinspired, Biomim. Nanobiomater. 5 (2016) 74–84.
[17] N. Thotakura, M. Dadarwal, P. Kumar, G. Sharma, S.K. Guru, S. Bhushan, K. Raza, O.P. Katare, Chitosan-Stearic acid based polymeric micelles for the effective delivery of tamoxifen: cytotoxic and pharmacokinetic evaluation, AAPS PharmSciTech (2016), http://dx.doi.org/10.1208/s12249-016-0563-6.
[18] R. Yang, W. Shim, F. Cui, G. Cheng, Enhanced electrostatic interaction between chitosan-modified PLGA nanoparticle and tumor, Int. J. Pharm. 371 (2009) 142–147.
[19] J.C. Moore, Gel permeation chromatography. I. a new method for molecular weight distribution of high polymers, J. Polym. Sci. Part A: Ploym. Chem. 2 (1964) 835–843.
[20] A. Bhatia, B. Singh, K. Raza, Tamoxifen-loaded lecithin organogel (LO) for topical application: development, optimization and characterization, Int. J. Pharm. 444 (2013) 47–59.
[21] H. Yadav, P. Kumar, V. Sharma, G. Sharma, K. Raza, O.P. Katare, Enhanced efficacy and better pharmacokinetic profile of tamoxifen employing polymeric micelles, RSC Adv. 6 (2016) 53351–53357.
[22] K. Raza, N. Thotakura, P. Kumar, M. Joshi, S. Bhushan, A. Bhatia, V. Kumar, R. Malik, G. Sharma, S.K. Guru, O.P. Katare, C60-fullerenes for delivery of docetaxel to breast cancer cells: a promising approach for enhanced efficacy and better pharmacokinetic profile, Int. J. Pharm. 495 (2015) 551–559.
[23] J. Koch-Weser, E.M. Sellers, Binding of drugs to serum albumin (first of two parts), N. Engl. J. Med. 294 (1976) 311–316.
[24] M.A. Rizvi, S. Guru, T. Naqvi, M. Kumar, N. Kumbhar, S. Akhoon, S. Banday, S.K. Singh, S. Bhushan, G. Mustafa Peerzada, B.A. Shah, An investigation of in vitro cytotoxicity and apoptotic potential of aromatic diselenides, Bioorg. Med. Chem. Lett. 24 (2014) 3440–3446.
[25] Y.-T. Xie, Y.-Z. Du, H. Yuan, F.-Q. Hu, Brain-targeting study of stearic acid-Grafted chitosan micelle drug-Delivery system, Int. J. Nanomed. 7 (2012) 3235–3244.
[26] Y. Chen, M. Schindler, S.M. Simon, A mechanism for tamoxifen-mediated inhibition of acidification, J. Biol. Chem. 274 (1999) 18364–18373.
[27] F.-Q. Hu, G.-F. Ren, H. Yuan, Y.-Z. Du, S. Zeng, Shell cross-linked stearic acid grafted chitosan oligosaccharide self-aggregated micelles for controlled release of paclitaxel, Colloids Surf. B Biointerfaces 50 (2006) 97–103.
[28] S. Chakravarthi, D. Robinson, Enhanced cellular association of paclitaxel delivered in chitosan-PLGA particles, Int. J. Pharm. 409 (2011) 111–120.
[29] L.-S. Wang, L.-C. Wu, S.-Y. Lu, L.-L. Chang, I.-T. Teng, C.-M. Yang, J.-A.A. Ho, Biofunctionalized phospholipid-capped mesoporous silica nanoshuttles for targeted drug delivery: improved water suspensibility and decreased nonspecific protein binding, ACS Nano 4 (2010) 4371–4379.
[30] F.-Q. Hu, X.-L. Wu, Y.-Z. Du, J. You, H. Yuan, Cellular uptake and cytotoxicity of shell crosslinked stearic acid-grafted chitosan oligosaccharide micelles encapsulating doxorubicin, Eur. J. Pharm. Biopharm. 69 (2008) 117–125.
[31] C.C. Benz, G.K. Scott, J.C. Sarup, R.M. Johnson, D. Tripathy, E. Coronado, H.M. Shepard, C.K. Osborne, Estrogen-dependent, tamoxifen-resistant tumorigenic growth of MCF-7Cells transfected with HER2/neu, Breast Cancer Res. Treat. 24 (1992) 85–95.